

Design of a Transmitarray Antenna Using 4 Layers of Double Square Ring Elements

Xian Wei Chua^{1, 2, *}, Tse-Tong Chia³, and Kerrell Boon Khim Chia³

Abstract—Conventional dielectric lenses rely on the accumulation of phase delay during wave propagation to produce a desired wavefront. By considering the required phase delay at each lens position, an ‘equivalent’ transmitarray antenna can be obtained. Despite a lack of curvature as in conventional lenses, the phase delay in the transmitarray antenna is achieved via a periodic arrangement of unit cell elements to bend the incident waves in the desired directions. This paper presents the design and characterization of a 4-layer transmitarray antenna consisting of double square ring elements. The gap between the double square rings is varied as a fixed proportion of their dimensions, while keeping the widths constant. The transmitarray element can achieve a transmission phase range of 235° with a loss of less than 3 dB. The performance of the transmitarray antenna is explicitly compared to that of a convex dielectric lens, both of which are operating at 8 GHz.

1. INTRODUCTION

Transmitarray antennae consist of planar, periodic arrays of printed circuit elements in sub-wavelength lattices. They have many advantages over conventional dielectric lenses for applications in satellite communication, automotive radar, and imaging systems: high-gain, lightweight, cheap, and small [1–7]. While zoning can reduce the weight of conventional lenses, it degrades system performance with reduced bandwidth and increased sidelobe levels [8]. Transmitarray antennae are also easier to fabricate with advancements in printed circuit board technologies [9, 10], while conventional lenses require expensive machining or molding processes [11]. Transmitarray antennae also have the major advantage of being planar, while conventional lenses can be bulky for the use in microwave antenna systems [12, 13]. Thus, transmitarray antennae are more portable, and easily integrated into systems or mounted onto platforms [5, 14]. The feed can also be positioned directly in front of the aperture without causing blockage losses [15, 16].

The general mechanism of a transmitarray antenna is to radiate the incident wave from a feed antenna, while incorporating a transmission phase shift at each element [17, 18]. Transmitarray antennae can be categorized into active and passive. In active transmitarray antennae, an external control signal is used for phase shift reconfiguration [15]. In passive transmitarray antennae, a variety of configurations exist in literature to adjust the phase of the incoming wave. These include identical microstrip patches of variable size or loaded with stubs of variable length, and elements connected through multiple layers by a delay line [16, 18, 19]. However, element placement can be challenging due to long lengths of line, and undesired modes or cross-polarized radiation may result [1]. A cascade of phase shifting layers, such as that presented in [1], can also be used. By treating each element as a Huygens source and altering its geometric parameters to locally modulate the transmission phase and amplitude [20], a transmitarray

Received 24 September 2020, Accepted 3 November 2020, Scheduled 17 November 2020

* Corresponding author: Xian Wei Chua (xwc21@cam.ac.uk).

¹ Cavendish Laboratory, University of Cambridge, Cambridge CB3 0HE, United Kingdom. ² A*STAR (Agency for Science, Technology and Research), Singapore 138632, Singapore. ³ DSO National Laboratories, Singapore 118230, Singapore.

can produce any arbitrary desired wavefront, and large freedom can be exercised when engineering its properties [13, 21].

Transmitarray antennae may resemble dielectric lenses in function, but their operation principles are different: dielectric lenses rely on the accumulation of phase delay by varying the thickness or refractive index [11, 22], while direct transmission and reflection are the sole propagating modes in transmitarray antennae [15].

This paper presents the design of a transmitarray antenna corresponding to a convex dielectric lens. In Section 2, the design of a convex dielectric lens operating at 8 GHz is presented using the ray analysis method of geometric optics. In Section 3, the design of a corresponding four-layer transmitarray antenna, using dual-resonant double square rings as unit cell elements, is presented. The gap between the rings is varied as a fixed proportion of their dimensions, while keeping the widths constant. This configuration is a variation of the variable-gap or variable-widths design in literature [1] and adds to our understanding of the behavior of double square ring elements. It is shown that the elements achieve a transmission phase range of 235° with a loss of less than 3 dB. In Section 4, the simulation results of both lenses are explicitly compared and discussed. Section 5 provides the conclusion and proposes future extensions.

2. DESIGN OF A CONVEX DIELECTRIC LENS

To focus a spherical wave from an electric dipole, each element on the lens must impart the required phase change [15, 22]. The phase delay experienced by a wave passing through a dielectric lens is given by [23, 24]:

$$\varphi(x, y) = kn\Delta(x, y) + k[\Delta_0 - \Delta(x, y)] = k\Delta_0 + k(n-1)\Delta(x, y) \quad (1)$$

where k is the wave number, n the refractive index, $\Delta(x, y)$ the thickness function, and Δ_0 the maximum thickness of lens.

The thickness function $\Delta(x, y)$ is given by [23, 24]:

$$\Delta(x, y) = \Delta_0 - R_1 \left(1 - \sqrt{1 - \frac{x^2 + y^2}{R_1^2}} \right) + R_2 \left(1 - \sqrt{1 - \frac{x^2 + y^2}{R_2^2}} \right) \quad (2)$$

where R_1 and R_2 are the radii of curvature of the left convex and right concave surfaces, respectively.

The focal length f of a thin lens is given by the Lensmaker's formula [25]:

$$\frac{1}{f} = (n-1) \left(\frac{1}{R_1} - \frac{1}{R_2} \right) \quad (3)$$

For an equiconvex lens ($R_1 = -R_2 = R$), the required phase delay as a function of the lens position is thus given by [17, 26]:

$$\varphi(x, y) = k\sqrt{\varepsilon_r\mu_r}\Delta_0 + 2k(\sqrt{\varepsilon_r\mu_r} - 1) \left[\sqrt{R^2 - x^2 - y^2} - R \right] \quad (4)$$

where $n = \sqrt{\varepsilon_r\mu_r}$, ε_r is the relative permittivity, and μ_r is the relative permeability.

For the focusing effect of a lens to be observed clearly, its diameter must be at least $10\lambda_0$, where λ_0 is the free-space wavelength. An operation frequency of 8 GHz, corresponding to $\lambda_0 = 3.75$ cm, is chosen for this study. For a conventional biconvex spherical dielectric lens with diameter of $12.8\lambda_0$ ($= 0.48$ m), $\varepsilon_r = 2.55$, $\mu_r = 1$, $\tan(\delta) = 0.01$, $\Delta_0 = 0.04$ m, $R = 1.45$ m and $F/D \approx 2.53$, the required phase range is 229° .

3. DESIGN OF AN 'EQUIVALENT' TRANSMITARRAY ANTENNA

3.1. Design of Unit Cell Element

A square loop element is chosen as it has a stable frequency response under various angles of incidence versus other elements such as cross-dipole [27–29]. Another concentric ring is added, with the inner ring loading the outer ring, to maximize the phase shift per layer and reduce the number of layers

required [30, 31]. In this double square ring element, the fundamental mode current distribution excited by a normally-incident, linearly-polarized wave is primarily concentrated on the ring sections parallel to the incident wave's polarization, and the transmitted wave should also be linearly polarized. As currents on the ring are oppositely directed, this presents the additional advantage of low cross-polarization [32].

To achieve the desired phase compensation value, the physical dimensions of the double square rings are varied around their resonant dimension. The geometrical model of the element, along with the design parameters, are shown in Figure 1.

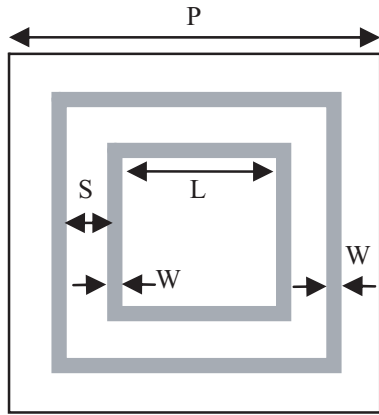


Figure 1. Design parameters of unit cell.

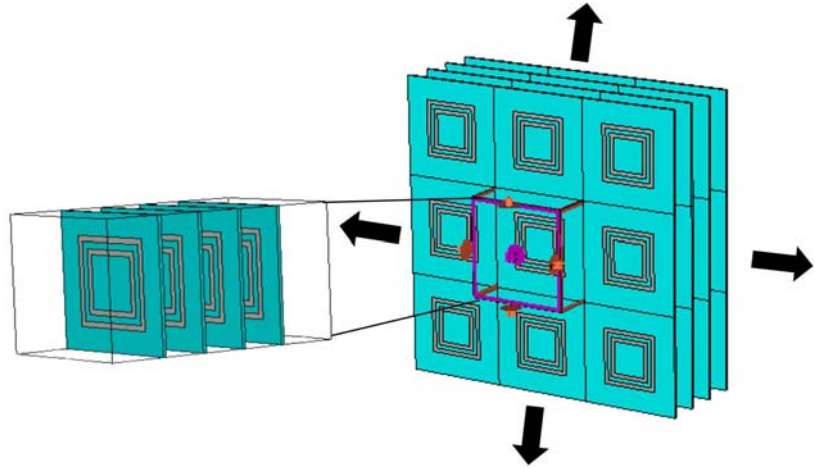


Figure 2. Four identical layers in a unit cell.

To reduce phase errors, the aim was to obtain a design S-curve with slow phase increment with respect to the geometrical dimensions of the unit cell element [1]. This is best accomplished by varying the gap S between the inner and outer rings, while keeping the length of the outer ring within the unit cell boundaries [1]. In addition, as a single layer transmitarray antenna cannot achieve the sufficient phase range coverage, multiple layers are required [33, 34]. In our study, we found that four identical layers, separated by an air gap, as shown in Figure 2, are required to achieve a full 360° phase range. This is consistent with a study by Abdelrahman, Elsherbeni and Yang [33].

Each layer is backed by a dielectric substrate. The values $\epsilon_r = 3$ and $T = 0.3$ mm were chosen for our unit cell. As a large periodicity is associated with increased sensitivity to variations of the angle of incidence and may cause grating lobes [2], the unit cell periodicity P was kept at $\lambda_0/3 = 12.5$ mm. A small periodicity also reduces the error resulting from discretization of the required phase profile [35] and avoids the generation of higher-order Floquet modes [11]. The simulation was run with the finite integration technique (FIT) in CST Microwave Studio [36]. A normal incidence plane wave was used to illuminate the unit cell element, and unit cell boundary condition was used to simulate an infinite array.

3.2. Properties of Unit Cell Element

Figure 3 depicts the transmission *phase* and *magnitude* of the unit cell element as a function of L , the dimension of the innermost ring, with periodicity $P = 12.5$ mm, loop width $W = 0.5$ mm, and loop separation $S = 0.125L$.

For the transmitarray antenna design, L of the innermost ring was varied between 0.983 and 4.904 mm. This avoids resonant dimensions associated with high transmission loss and maintains loss below 2.32 dB to ensure high aperture efficiency.

3.3. Design Configurations of Dielectric Lens and Transmitarray Antenna

For the design of the transmitarray antenna, only the phase shift at the center of unit cells was considered. Figure 4 shows the ideal phase profile in the dielectric lens, and the corresponding discretized

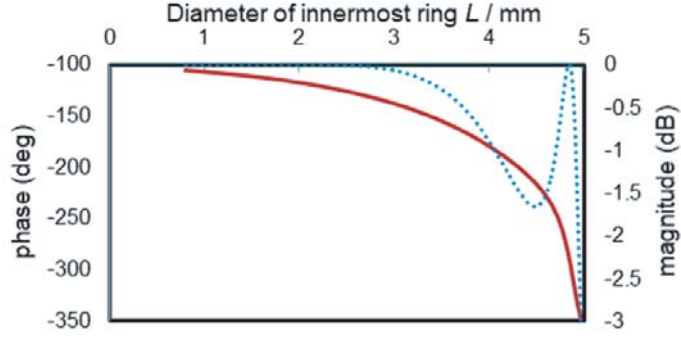


Figure 3. Graph of transmission phase (red, solid) and magnitude (blue, dotted) against L of innermost ring at 8 GHz.

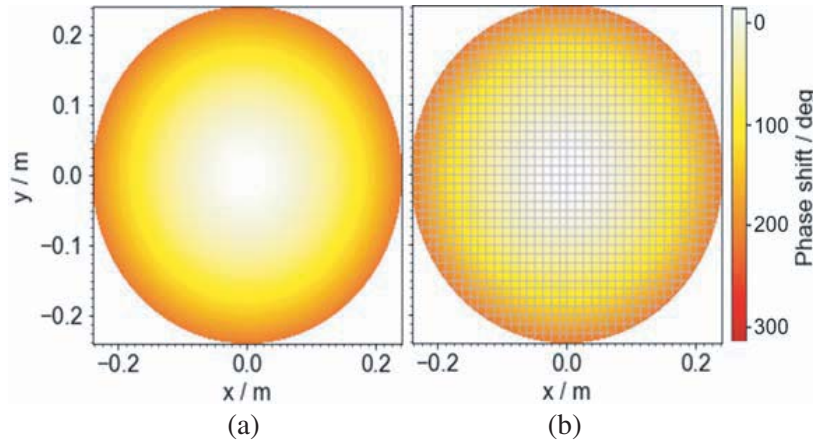


Figure 4. Phase profile for (a) convex dielectric lens and (b) transmitarray antenna.

Table 1. Design configuration of convex dielectric lens.

Parameter	Value
Radius of Curvature of Spherical Surfaces (R) / cm	145
Maximum Thickness (Δ_0) / cm	4
Substrate Permittivity (ϵ_r)	2.55
Dielectric Loss Tangent	0.01
Aperture Diameter / cm	48
Feed to Diameter Ratio (F/D)	2.53
Focal Length (f) / cm	121.47

phase profile in the transmitarray antenna. Both lenses were illuminated by an electric dipole placed at $f = 121.47$ cm. The design configurations of both the convex dielectric lens and the transmitarray antenna are presented in Tables 1 and 2, respectively. Figure 5 shows the design of the transmitarray antenna. A comparison with the design of other transmitarray antennae in literature also utilizing a double square ring element is presented in Table 3 [1, 32, 37–39].

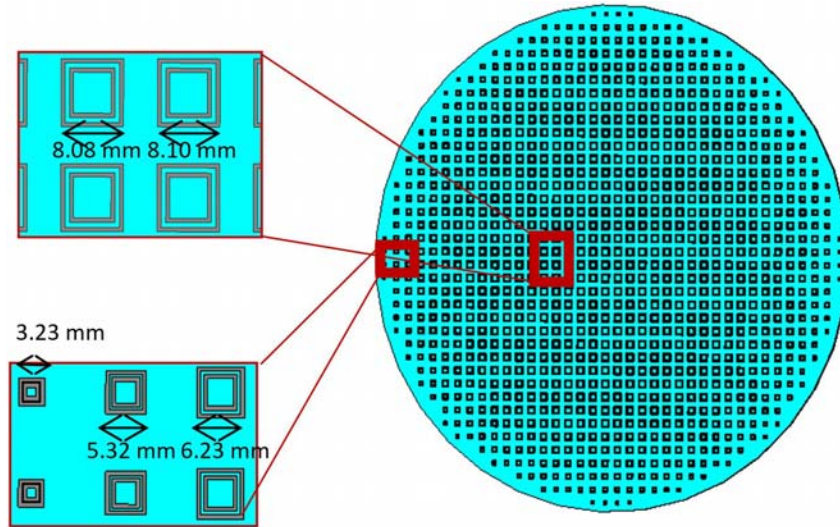


Figure 5. Transmitarray antenna design.

Table 2. Design configuration of transmitarray antenna.

Parameter	Value
Number of Conductor Layers	4
Substrate Thickness (T) / mm	0.3
Substrate Permittivity (ϵ_r)	3
Layer Separation / mm	3.7
Unit Cell Periodicity (P) / mm	12.5
Number of Elements Per Layer	1076
Inner Loop Diameter / mm	0.983–4.904
Aperture Diameter / cm	48
Feed to Diameter Ratio (F/D)	2.53
Loop Width (W) / mm	0.5
Loop Separation (S)	$0.125L$

4. CORRELATION AND COMPARISON OF PERFORMANCE

The simulation results are presented in this section. The phase and amplitude plots of the E-field for both the convex dielectric lens and transmitarray antenna in the $x = 0$ plane are presented in Figure 6 and Figure 7, respectively. Videos of the simulation are available online.

In both cases, the focusing effect is clearly observable and similar, validating the design of the transmitarray antenna. However, there is a greater spread of energy for the transmitarray antenna. The discrepancies can be attributed to two main factors: firstly, the infinite array simulation assumes similar coupling between neighboring elements. In reality, the coupling increases with distance from the center, thus altering approximate phases. Furthermore, the transmitarray antenna is finite-sized, giving rise to diffraction at the edges [32]. Secondly, the simulation assumes a normally-incident plane wave on all elements of the transmitarray antenna. In reality, most elements are illuminated by oblique angles θ [17, 40, 41]. This reduces their effective dimensions by $\cos\theta$, altering the current induced. This is an important factor for small F/D lenses [11].

Table 3. Comparison of the proposed transmitarray antenna to some existing transmitarray antennae.

Ref.	Freq. (GHz)	Unit Cell Element	Varying Parameters	Constant Parameters	No. of Layers	Array Size (λ_0^2)	Transmission Phase Range (deg)	Transmission Magnitude (dB)
[1]	30	Double square ring	1) Gap between rings 2) Width of outer ring	1) Width of outer ring 2) Gap between rings	4	12.6×12.6	1) 312 2) 329	1) > -3.0 2) > -2.0
[32]	30	Double square ring	Width of inner ring	Width of outer ring	4	12.6×12.6	270	> -3.0
[37]	12	Outer Layers: Cross slots; Middle Layer: double square ring	Dimension of both rings and gap between rings	Width of both rings	3	$\pi \times (4.4)^2$	> 360	> -3.7
[38]	10	Double square ring with center patch	Dimension of outer ring	Width of both rings and gap between rings	4	7.5×7.5	> 360	> -1.2
This Work	8	Double square ring	Dimension of both rings and gap between rings	Width of both rings	4	$\pi \times (6.4)^2$	235	> -3.0

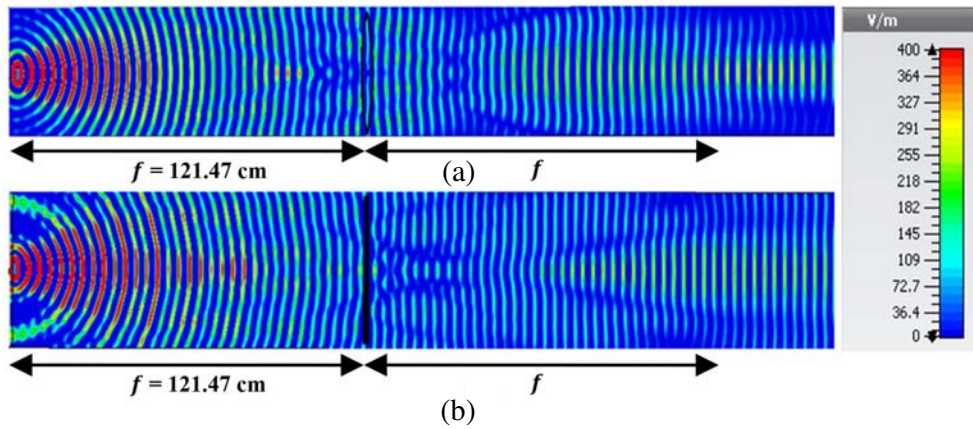


Figure 6. Phase plot of E-field of (a) convex dielectric lens and (b) transmitarray antenna at $x = 0$ plane.

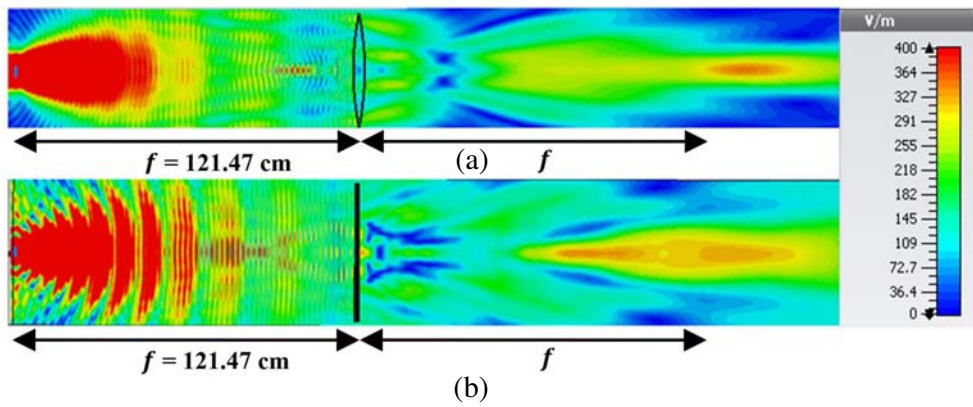


Figure 7. Amplitude plot of E-field of (a) convex dielectric lens and (b) transmitarray antenna at $x = 0$ plane.

5. CONCLUSION

In conclusion, this paper presents and compares the performance of a conventional lens antenna and an 'equivalent' transmitarray antenna. A convex dielectric lens operating at 8 GHz has been proposed using geometric optics, and a corresponding transmitarray antenna consisting of double square loop elements was designed. Our simulation shows that the proposed transmitarray antenna mimics the original convex lens, validating our design methodology, while having additional merits of a flat and thin profile, and easier fabrication. Our study adds to the understanding of the behaviour of double square ring elements.

For further work, our unit cell element can be analyzed using an equivalent-circuit model. This allows rapid computation of the frequency response, for complex elements like the double square ring used, where large numbers of current modes are required [42, 43]. This will serve to design broader bandwidth and multiple bands transmitarray antennae for applications in satellite communication, automotive radar, and imaging systems.

ACKNOWLEDGMENT

Commercial software CST Microwave Studio was used for the simulations presented. X. W. Chua would also like to thank Dr. Tan Guoxian of Raffles Institution, Singapore, for consultations and support.

REFERENCES

1. Ryan, C. G. M., J. R. Brag, and Y. M. M. Antar, "A broadband transmitarray using double square ring elements," *13th Int. Symp. on Antenna Technol. and Appl. Electromagnetics and the Canadian Radio Sciences Meeting*, 2009.
2. Nematollahi, H., J. J. Laurin, J. E. Page, and J. A. Encinar, "Design of broadband transmitarray unit cells with comparative study of different numbers of layers," *IEEE Trans. Antennas Propag.*, Vol. 63, No. 4, 1473–1481, Apr. 2015.
3. Frost, C., "Measurement notes: Measurement and evaluation of artificial dielectric material," *Pulse Power Physics*, Apr. 2012.
4. Zainud-Deen, S. H., W. M. Hassan, and K. H. Awadalla, "Radiation characteristics enhancement of dielectric resonator antenna using solid/discrete dielectric lenses," *Advanced Electromagnetics*, Vol. 4, No. 1, Feb. 2015.
5. Kaouach, H., L. Dussopt, R. Sauleau, and T. Koleck, "Design and demonstration of an X-band transmit-array," *2009 3rd European Conference on Antennas and Propagation*, 1191–1195, Berlin, 2009.
6. Zhou, S. N., Z. B. Wang, and Y. J. Feng, "Optimal design of wideband radar absorbing structure consisting of resistive meta-surface layers," *2012 International Conference on Microwave and Millimeter Wave Technology (ICMMT)*, 1–4, Shenzhen, 2012.
7. Guo, Y. J. and S. K. Barton, "Flat printed lens and reflector antennas," *1995 Ninth International Conference on Antennas and Propagation, ICAP '95 (Conf. Publ. No. 407)*, Vol. 1, 253–256, Eindhoven, Netherlands, 1995.
8. Proudfoot, P., O. H. Dayton, M. Mehalic, and A. Terzouli, "Design and testing of a lightweight, planar microwave lens," *Proc. IEEE Antennas Propag. Soc. Int. Symp.*, Vol. 1, 495–498, 1992.
9. Wang, Y., H. Deguchi, and M. Tsuji, "A broadband flat lens based on aperture-coupled patch FSSs with four-pole resonant behaviour," *Proc. IEEE Antennas Propag. Soc. Int. Symp.*, 1–2, Chicago, IL, 2012.
10. Ali, T., I. Bendoyim, S. Kaceniari, A. Golovin, and D. Crouse, "Metamaterials lens design for microwave," Retrieved from <http://metaconferences.org/ocs/public/conferences/9/pdf/3543.pdf>.
11. Gagnon, N., "Phase Shifting Surface (PSS) and Phase and Amplitude Shifting Surface (PASS) for microwave applications," Ph.D. dissertation, School of Information Technology and Engineering, University of Ottawa, Canada, 2011.

12. Silver, S., *Microwave Antenna Theory and Design*, Institution of Engineering and Technology, London, UK, 1949.
13. Wang, Z., J. Chen, and M. Xue, "Terahertz lenses based on nonuniform metasurfaces," *Optics Communications*, Vol. 338, 585–589, Nov. 2015.
14. Lau, J. Y., "Reconfigurable transmitarray antennas," Ph.D. dissertation, Dep. Elect. and Comp. Eng., University of Toronto, Canada, 2012.
15. Shaker, J., "Natural and artificial dielectrics: Similarities and differences," *Antenna Technology and Applied Electromagnetics & the American Electromagnetics Conference 14th International Symposium*, 2010.
16. Zainud-Deen, Sr., S. M. Gaber, H. A. Malhat, and K. W. Awadalla, "Single feed dual-polarization dual-band transmitarray for satellite applications," *30th National Radio Science Conference*, 27–34, Apr. 2013.
17. Abdelrahman, H., A. Z. Elsherbeni, and F. Yang, "High-gain and broadband transmitarray antenna using triple-layer spiral dipole elements," *IEEE Antennas Wireless Propag. Lett.*, Vol. 13, 1288–1291, 2014.
18. Erdil, E., K. Topalli, O. Zorlu, and T. Toral, "A reconfigurable microfluidic transmitarray unit cell," *7th European Conference on Antennas and Propagation*, 2957–2960, Apr. 2013.
19. Rajagopalan, H. and Y. Rahmat-Samii, "Reflectarray antennas: An intuitive explanation of reflection phase behavior," *XXXth URSI, General Assembly and Scientific Symposium*, 1–4, 2011.
20. He, Y. and G. V. Eleftheriades, "Rotated infrared antenna transmitarray for the manipulation of circularly polarized wavefronts," *EPJ Appl. Metamat.*, Vol. 1, No. 8, 2014.
21. Neu, J., B. Krolla, O. Paul, B. Reinhard, R. Beigang, and M. Rahm, "Metamaterial-based gradient index lens with strong focusing in the THz frequency range," *Opt. Express*, Vol. 18, No. 26, 22748–22757, Dec. 2010.
22. Monticone, F., N. M. Estakhri, and A. Alu, "Manipulating the nanoscale optical transmission with a meta-transmitarray," Feb. 2013, Retrieved from <http://arxiv.org/abs/1302.6260>.
23. Goodman, J., *Introduction to Fourier Optics*, 3rd Edition, Roberts & Company, Englewood, Colorado, USA, 2005.
24. Ersoy, O., *Diffraction, Fourier Optics and Imaging*, John Wiley & Sons, Hoboken, NJ, USA, 2006.
25. Hecht, E., *Optics*, 149–165, 4th Edition, Addison Wesley, San Francisco, 2002.
26. Abdelrahman, H., P. Nayeri, A. Z. Elsherbeni, and F. Yang, "Bandwidth improvement methods of transmitarray antennas," *IEEE Trans. Antennas Propag.*, Vol. 63, No. 7, 2946–2954, Jul. 2015.
27. Guha, D. and Y. M. M. Antar, *Microstrip and Printed Antennas: New Trends, Techniques and Applications*, Wiley, Hoboken, NJ, USA, 2010.
28. Sulaiman, H. A., M. A. Othman, M. Z. A. Abd Aziz, and M. F. Abd Malek (Eds.), *Theory and Applications of Applied Electromagnetics*, Springer, Switzerland, 2014.
29. Sulaiman, H. A., M. A. Othman, M. F. I. Othman, Y. Rahim, and C. P. Naim, "Double square loop frequency selective surface for GSM shielding," *Advanced Computer and Communication Engineering Technology*, Springer, Switzerland, 2015.
30. Shaker, J., M. R. Chaharmir, and J. Ethier, *Reflectarray Antennas: Analysis, Design Fabrication and Measurement*, Artech House, Norwood, MA, USA, 2013.
31. Chaharmir, M. R., J. Shaker, M. Cuhaci, and A. Ittipiboon, "A broadband reflectarray antenna with double square rings," *Microw. Opt. Technol. Lett.*, Vol. 48, No. 7, 1317–1319, Jul. 2006.
32. Ryan, C. G. M., M. R. Chaharmir, J. Shaker, J. R. Bray, Y. M. M. Antar, and A. Ittipiboon, "A wideband transmitarray using dual-resonant double square rings," *IEEE Trans. Antennas Propag.*, Vol. 58, No. 5, 1486–1493, May 2010.
33. Abdelrahman, H., A. Z. Elsherbeni, and F. Yang, "Transmission phase limit of multilayer frequency-selective surfaces for transmitarray designs," *IEEE Trans. Antennas Propag.*, Vol. 62, No. 2, 690–697, Feb. 2014.
34. Abdelrahman, H., A. Z. Elsherbeni, and F. Yang, "Transmission phase limit of multilayer frequency-selective surfaces for transmitarray designs," *IEEE Trans. Antennas Propag.*, Vol. 62, No. 2, 690–

- 697, Feb. 2014.
35. Nematollahi, H. and J. J. Laurin, "Reconfigurable reflector antenna based on transmit-array feeding system with a study on the phase discretization of the transmit-array," *Proc. 30th Int. Commun. Satell. Syst. Conf.*, 1–7, Ottawa, Canada, Sept. 2012.
 36. CST Microwave Studio, [Online], Available: <http://www.cst.com>.
 37. Tian, C., Y. Jiao, G. Zhao, and H. Wang, "A wideband transmitarray using triple-layer elements combined with cross slots and double square rings," *IEEE Antennas and Wireless Propagation Letters*, Vol. 16, 1561–1564, 2017.
 38. Zhu, H., L. Guo, and W. Feng, "A transmitarray antenna employing double square ring slot unit cells without dielectric substrate," *2019 International Workshop on Electromagnetics: Applications and Student Innovation Competition (iWEM)*, 1–2, Qingdao, China, 2019.
 39. Muhammad, M., et al., "Wideband multi-layer frequency selective surface based transmitarray unit cell for satellite communication applications," *2019 International Symposium on Antennas and Propagation (ISAP)*, 1–3, Xi'an, China, 2019.
 40. Plaza, E. G., G. Leon, S. Loredó, and F. Lan-Heras, "A simple model for analyzing transmitarray lenses," *IEEE Trans. Antennas Propag.*, Vol. 57, No. 2, 131–144, Apr. 2015.
 41. Khalizadeh, M. and M. M. Mirsalehi, "Design of a microwave dual-band filter using frequency selective surfaces," *20th Iranian Conference on Electrical Engineering*, 2012.
 42. Lee, K. and R. J. Langley, "Equivalent-circuit models for frequency-selective surfaces at oblique angles of incidence," *IEE Proceedings H — Microwaves, Antennas and Propagation*, Vol. 132, No. 6, 395–399, Oct. 1985.
 43. Langley, R. J. and E. A. Parker, "Double-square frequency-selective surfaces and their equivalent circuit," *Electronics Letters*, Vol. 19, No. 17, 675–677, Aug. 18, 1983.